Supplementary Information

Green and Efficient Recovery of Mo, Ni, and V from Spent Residue Hydrotreating Catalysts with Deep Eutectic Solvents

Xinran Fu[a], Xiaoning Cao[a], Ruinian Xu[a], Ke Xu[b], Huandi Hou[b,], Zijun Wang[b], Chengna Dai[a,*] and Biaohua Chen[a]*

[a] College of Environmental Science and Engineering, Beijing University of Technology, Beijing, 100124, China

[b] Laboratory of Heavy Oil Processing, Sinopec Research Institute of Petroleum Processing, Beijing 100083, China

[*]**Corresponding author. Email**: houhd.ripp@sinopec.com (H. Hou), daicn@bjut.edu.cn (C. Dai).

Experimental section

Chemicals

The spent residue hydrotreating catalysts was supplied by Zhejiang Petrochemical Co., Ltd. and used as received without calcination. Before leaching experiments, the catalyst was dried at 60℃ for 1 h. All chemicals used in the experiments were of analytical grade and employed without further purification. Choline chloride (ChCl, $C_5H_{14}ClNO$, ≥98%) and ethylene glycol (EG, $C_2H_6O_2$, ≥99%) were purchased from Shanghai Aladdin Biochemical Technology Co., Ltd. Urea (CH_4N_2O, ≥99%), p-toluenesulfonic acid (PTSA, $C_7H_8O_3S$; ≥99%), and betaine Hydrochloride (BCl, $C_5H_{11}NO_2 \cdot Cl$; ≥99%) were purchased from Shanghai Maclin Biochemical Technology Co., Ltd. Hydrochloric acid (HCl) and nitric acid (HNO_3) were obtained from Shanghai Bide Medical Technology Co., Ltd. Benzenesulfonic acid monohydrate (BSAM, $C_6H_8O_4S$, ≥98%) were purchased from Adamas Co., Ltd. L-Carnitine hydrochloride (LC-HCl, $C_7H_{16}O_3NCl$, ≥98%) was obtained from Shanghai Dibai Biotechnology Co., Ltd. Standard solutions of Mo, V, and Ni (each 1000 $mg \cdot L^{-1}$) were purchased from the National Analysis & Testing Center for Nonferrous Metals & Electronic Materials Co., Ltd.

Synthesis of Deep Eutectic Solvents (DESs)

The deep eutectic solvents (DESs) were synthesized by combining hydrogen bond acceptors (HBAs) and hydrogen bond donors (HBDs) at predetermined molar ratios. In a typical procedure, the designated amounts of HBA and HBD were mixed in a 20 mL glass vial. The mixture was heated in a thermostated water bath maintained at 70°C under continuous magnetic stirring until a clear, homogeneous liquid formed, indicating complete DES

formation. The resulting DES was cooled to room temperature and stored in sealed vials for subsequent leaching experiments.

Leaching experiments

Leaching experiments were conducted using a conventional hydrometallurgical approach, as outlined in **Fig. S1**. Typically, 0.1 g of the dried spent catalyst was added into 5 mL of DES in a glass vial, and the mixture were stirred in a thermostated water bath for 48 h. The recovery efficiencies of Mo, Ni, and V with various DESs was examined, and the most effective DES was selected for further optimization. After leaching, the solutions were diluted with distilled water and dilute nitric acid prior to inductively coupled plasma (ICP) analysis. The leaching efficiency was calculated according to the following Eq. (**S1**):

$$\text{Leaching efficiency} = C \times V_{\text{DES}} / m \times 100 \quad \text{(S1)}$$

where C is the final metal concentration in the solution ($mg \cdot L^{-1}$), V_{DES} is the volume of the initial leaching solution (L), and m is the mass of metal in the solid feed (mg). The effects of temperature, time and solid-liquid ratio on the leaching process were investigated.

Characterization

The metal content in the spent residue hydrotreating catalysts was determined by inductively coupled plasma optical emission spectroscopy (ICP-OES, PerkinElmer Optima 5300DV; 1.5 kW, 40.68 MHz). Before analysis, the catalyst sample was completely digested in a mixture of HNO_3 and HCl (v/v=1:3), and the resulting solution was diluted with deionized water.

Powder X-ray diffraction (XRD) patterns were collected on a Bruker D8-Advance diffractometer with Cu Kα radiation. Scans were recorded from 5° to 80° (2θ) at a rate of

5°/min. The morphological features of the spent catalyst before and after leaching were examined by scanning electron microscopy (SEM, ZEISS GeminiSEM 300).

Surface chemical properties were probed by Fourier-transform infrared spectroscopy (FT-IR, B420-Bruker). Powder samples were loaded directly into the FT-IR cell without dilution. Spectra were acquired in the range of 4000-500 cm^{-1} at a resolution of 2 cm^{-1} by accumulating 64 scans, with pure KBr used as the background reference.

^{1}H nuclear magnetic resonance (NMR) spectra were recorded on an Ascend TM 600 spectrometer (Avance HD III) using deuterated dimethyl sulfoxide (DMSO-d_6) as the solvent and external reference. NMR was used to determine the compositions of the DESs and their individual components before and after leaching.

The viscosity of ChCl-3BSAM was measured using a microviscometer (Lovis 2000ME, Anton Paar). The sample was loaded without dilution, and the measurements were conducted at ambient pressure over a temperature range of 20-35^{o}C, with data points recorded at 5^{o}C intervals.

DFT computational details

Based on first-principles calculations, we employed the Vienna Ab initio Simulation Package (VASP, 5.4.4) within the framework of density functional theory (DFT).[1] The projector-Augmented-Wave (PAW) method and Perdew-Burke-Ernzerhof (PBE) exchange-correlation functional under the generalized gradient approximation (GGA) were used to investigate the surface reaction mechanisms and electronic structures. A plane-wave basis set with a kinetic energy cutoff of 500 eV was adopted. The partial occupancies of the Kohn-Sham orbitals were treated using the Gaussian smearing method with a width of 0.05 eV. Structural

optimization and energy calculations were performed using a T-centered 1×1×1 k-point mesh to sample the Brillouin zone. All atomic geometries and total energies were converged to within 10^{-5} eV to ensure the computational accuracy. Based on the comprehensive characterization results, structural models of the spent residue hydrotreating catalysts, HBAs, HBDs used in the experiment, and various synthesized DESs were constructed, and the adsorption energy between the spent residue hydrotreating catalysts and various DESs were calculated. Frontier molecular orbital (FMO) analysis, charge density difference mapping, and Bader charge analysis were conducted to elucidate electron transfer behavior and interaction mechanisms between the spent catalyst and DESs.

Initial molecular models were built in Materials Studio (MS) and geometrically optimized using VASP. To identify reactive sites, the electrostatic potential (ESP) distributions of the HBAs and HBDs were computed using the accurate molecular orbital tools available in MS.

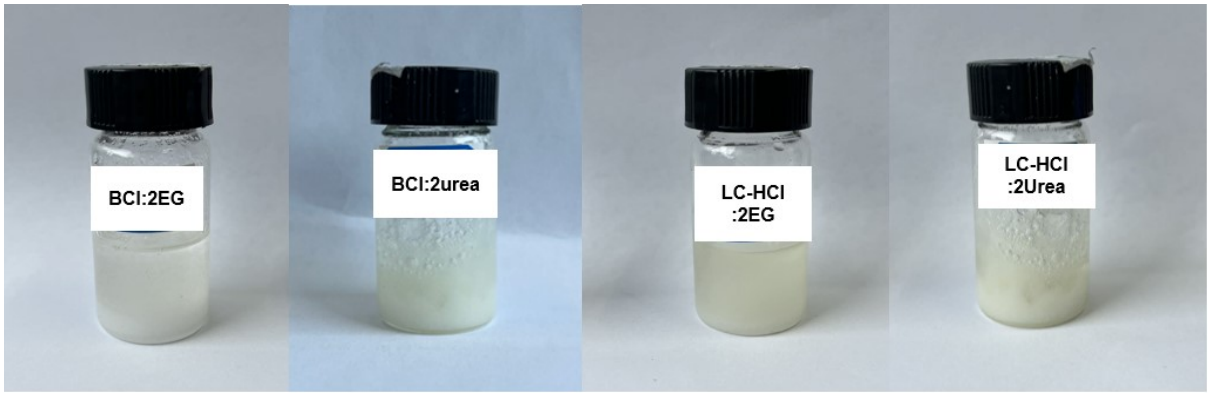

Fig. S1. Photos of the un-stable DESs

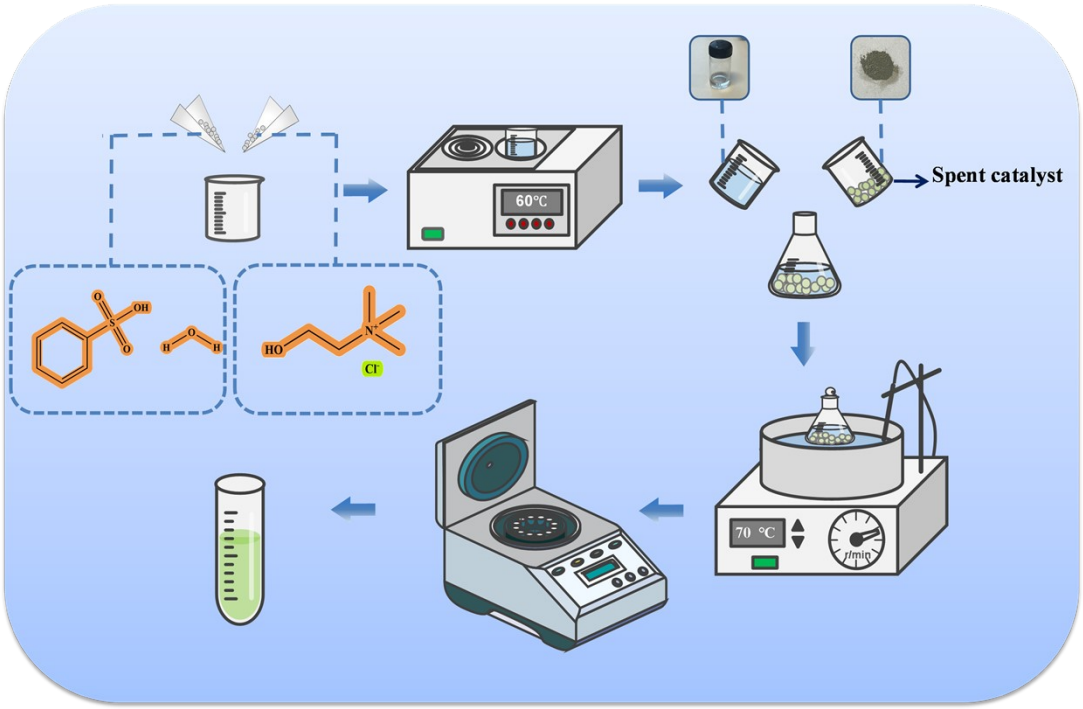

Fig. S2. Schematic diagram of DES preparation and Leaching Experiment Process.

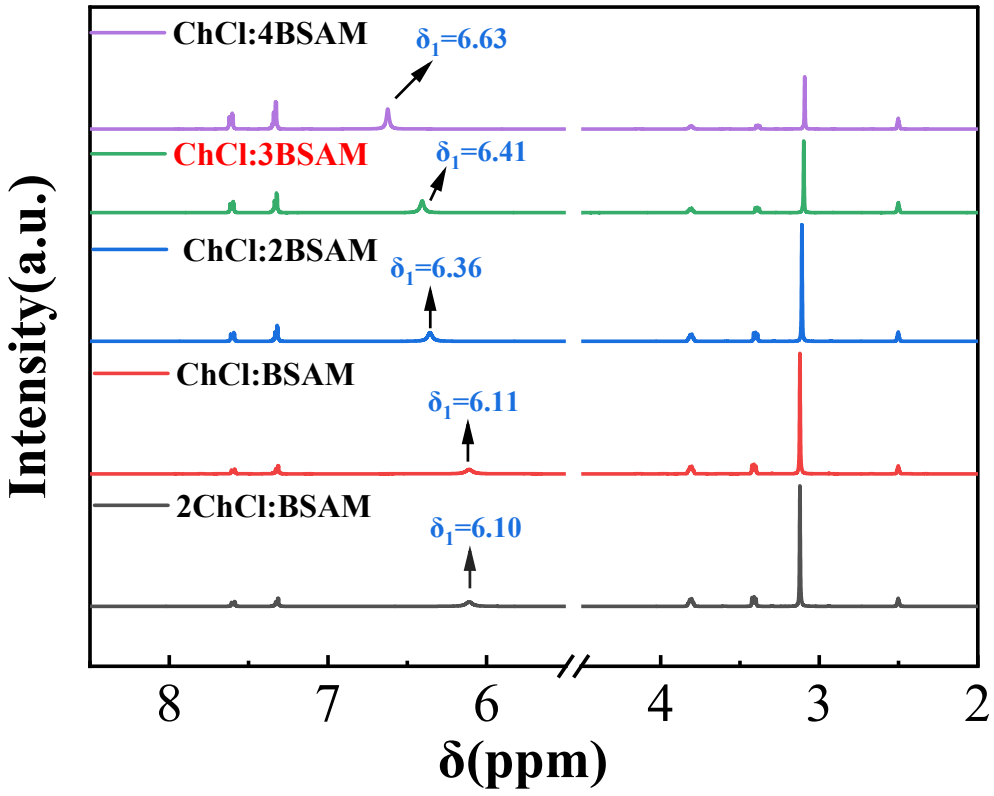

Fig. S3. ^{1}H NMR spectra of ChCl and BSAM with different molar ratios.

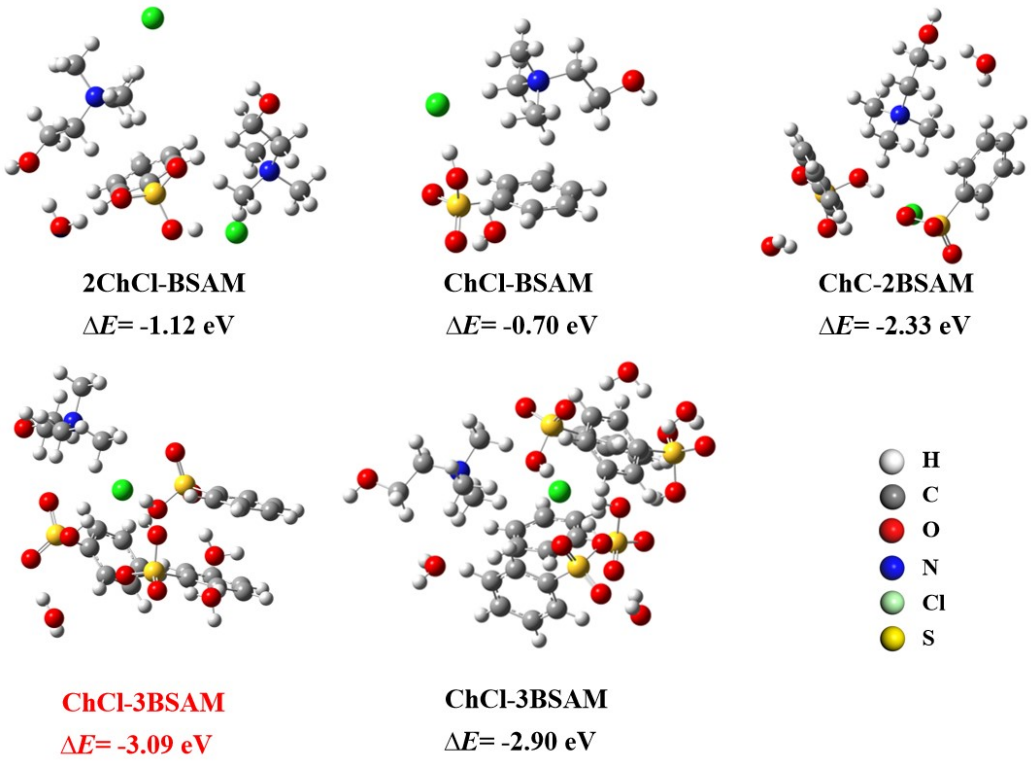

Fig. S4. The binding energies of ChCl and BSAM in different molar ratios.

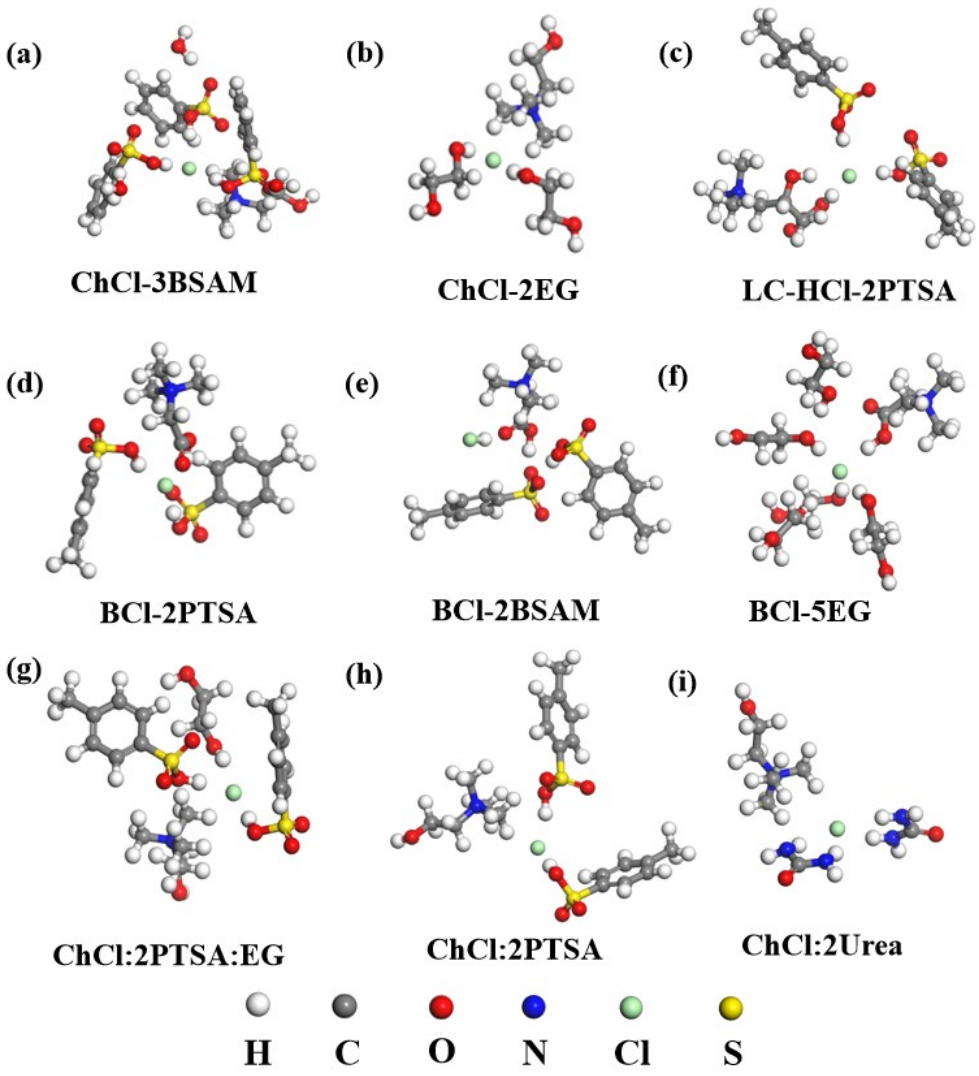

Fig. S5. (a)-(i) Clustered Structure Model of DESs Prepared in the Experiment.

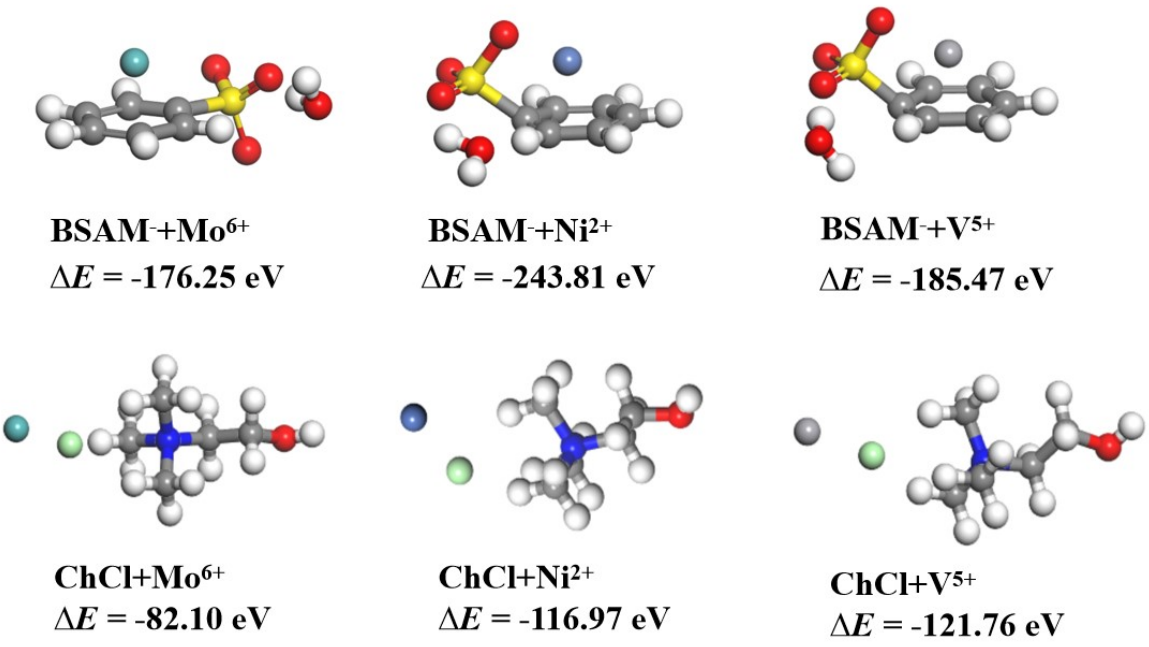

Fig. S6. The binding energies of Mo^{6+}, Ni^{2+}, and V^{5+} with BSMA and ChCl, respectively.

Table S1. HBA, HBD, and the ability to synthesize DES

HBA	HBD	DES
betaine hydrochloride	2ethylene glycol	×
betaine hydrochloride	5ethylene glycol	√
betaine hydrochloride	2benzenesulfonic acid monohydrate	√
betaine hydrochloride	2p-toluenesulfonic acid	√
betaine hydrochloride	2urea	×
L-carnitine hydrochloride	2ethylene glycol	×
L-carnitine hydrochloride	2benzenesulfonic acid monohydrate	√
L-carnitine hydrochloride	2p-toluenesulfonic acid	√
L-carnitine hydrochloride	2urea	×
choline chloride	2ethylene glycol	√
choline chloride	2benzenesulfonic acid monohydrate	√
choline chloride	2p-toluenesulfonic acid	√
choline chloride	2p-toluenesulfonic acid-ethylene glycol	√
choline chloride	2urea	√

Table S2. ICP analysis of metal loadings in catalysts.

Elemental	Content%
Mo	31.78%
Ni	4.78%
V	16.60%

Table S3. Density and dynamic viscosity of DES1 at different temperatures.

Temperature/^{o}C	Density/g·cm^{-2}	Dynamic viscosity/mPa·s
20	1.29	234.18
25	1.29	184.31
30	1.28	142.23
35	1.28	105.04
40	1.28	91.07

Table S4. Leaching conditions and leaching rates of Mo, Ni, and V in catalysts extracted from different solvent systems.

Novel solvent	Valuable metal content in raw materials (wt %)	Leaching conditions	Leaching results	Ref.
ChCl-3BSAM	Mo = 31.78, Ni = 4.78, V = 16.60	T = 80°C, t = 420 min, S/L = 1:20 g·mL^{-1}	Selective leaching Mo (99.2%), Ni (90.72%), V (93.61 %)	This work
Ionic liquid Aliquat336	Mo = 18.17, Ni = 12.19, V = 39.51	C = 0.1 mol·L^{-1}, H_2O_2 to Aliquat336 = 20% (v/v), T = 60°C, t = 120 min	Selective leaching Mo (69.5%), Ni (≈13%), V (82.1%)	2
Ali-D2	Mo = 18.17, Ni = 12.19, V = 39.51	C = 0.4 mol·L^{-1}, H_2O_2 to ALiD2=40% (v/v), T = 60°C, t = 150 min	Selective leaching Mo (70%), Ni (≈10%), V (83.2 %)	2
cy-D2EH	Mo = 5.40, Ni = 8.9, V = 25.8	C = 0.3 mol·L^{-1}, H_2O_2 to cy-D2EH = 30% (v/v), T = 50°C, t = 120-180 min	Selective leaching Mo (82.5%), Ni (≈10%), V (91%)	3
PhCl-PTSA-EG	Mo = 0.9, Ni = 7.7, V = 3.1	T = 100°C, t = 1440 min, S/L = 1:50 g·mL^{-1},	Non-selective Ni (81%)	3
ChCl-OA	Mo = 5.43, Ni = 5.03, V = 7.98	T = 80°C, t = 180 min, S/L = 1:20 g·mL^{-1}	Selective leaching Mo (95.1%), Ni (1.8%), V (97.8%)	4

Table S5. Frontier molecular orbital energies of $NiMoO_4$ and DESs.

	HOMO/eV	**LUMO/eV**	**ΔE_1/eV**	**ΔE_2/eV**
$NiMoO_4$	-4.195626	-1.301049	/	/
ChCl-3BSAM	-5.587298	-1.589515	2.606111	4.286249
ChCl-2EG	-4.384698	-0.961950	3.233676	3.083649
LC-HCl-2PTSA	-4.886198	-0.998229	3.197397	3.585149
BCl-2PTSA	-4.863936	-0.921985	3.273641	3.562887
BCl-2BSAM	-4.886198	-0.998220	3.406714	3.188352
BCl-5EG	-4.489401	-0.788912	3.374373	3.471325
ChCl-2PTSA-EG	-4.772374	-0.821253	3.39415	3.912974
ChCl-2PTSA	-5.070831	-1.084073	3.111553	3.769782
ChCl-2Urea	-4.363462	-0.890464	3.197397	3.585149

Table S6. Adsorption energy table of DES1 on $NiMoO_4$.

DESs	Oxide	Binding Energy(eV)
ChCl-3BSAM	$NiMoO_4$	-3.77
ChCl-2EG	$NiMoO_4$	-0.36
LC-HCl-2PTSA	$NiMoO_4$	-0.49
BCl-2PTSA	$NiMoO_4$	-0.33
BCl-2BSAM	$NiMoO_4$	-1.44
BCl-5EG	$NiMoO_4$	-0.32
ChCl-2PTSA-EG	$NiMoO_4$	-0.98
2ChCl-PTSA	$NiMoO_4$	-1.86
ChCl-2Urea	$NiMoO_4$	-2.03

Reference

1 V. Wang, N. Xu, J. C. Liu, G. Tang and W.-T. Geng, *Comput. Phys. Commun.*, 2021, **267**, 108033.

2 T. T. Tran, Y. Liu and M. S. Lee, *Sep. Purif. Technol*, 2021, **255**, 117734.

3 Z. Abbas and S. M. Jung, *Sep. Purif. Technol*, 2024, **346**, 127450.

4 J. Chen, S. Sun, X. Luo, F. Xiao, J. Chen, Z. Yang, C. Sui, K. Yu and G. Tu, *J. Environ. Chem. Eng.*, 2025, **13**, 117123.